PHYSICAL REVIEW B VOLUME 48, NUMBER 13 1 OCTOBER 1993-I

Doping- and pressure-induced change of electrical and magnetic properties in the Mott-Hubbard insulator $LaTiO_3$

Y. Okada, T. Arima, and Y. Tokura*
Department of Physics, University of Tokyo, Tokyo 113, Japan

C. Murayama and N. Môri
Institute for Solid State Physics, University of Tokyo, Tokyo 106, Japan

(Received 29 March 1993; revised manuscript received 28 June 1993)

A perovskitelike compound $LaTiO_3$ shows insulating or barely metallic behavior depending on a slight (≤ 0.04) deviation of the Ti valence (+3) arising from nonstoichiometry of La and/or oxygen. In order to investigate electronic properties of the specimens in the very vicinity of the Mott insulator-metal phase boundary, we have measured the doping- and pressure-induced effects on the electrical and magnetic properties. The results have indicated a crossover behavior from localized to itinerant nature of the electronic state with increase of the doping level and one-electron bandwidth.

I. INTRODUCTION

Change of the band filling in Mott-Hubbard insulators leads, in general, to the metallic states via collapse of the spin-ordered phase at low temperatures. One of the prototypical examples is the layered cuprates, which show a transitional behavior of the electronic ground state from the antiferromagnetic insulator to normal metal via the high-T_c superconductor when the band filling is changed from half-filling.[1,2] Apart from recent extensive studies on these doped cuprates, however, not so much has been known about the doping-induced insulator-metal transition in Mott-Hubbard systems. The $LaTiO_3$ system investigated here may be one of the most appropriate systems for such a study, as demonstrated in the following.

According to the Zaanen-Sawatzky-Allen scheme,[3] correlated insulators in transition metal oxide systems can be categorized to either the Mott insulator or the charge-transfer (CT) insulator, in which the minimum charge gap is formed between the lower and upper Hubbard bands (d electron band) or between the occupied O $2p$ band and upper Hubbard band, respectively. The parent compounds of the cuprate superconductors are typical CT insulators with $3d^9$ configuration (i.e., one d hole per Cu site). By contrast, the $LaTiO_3$ system can be viewed as a Mott insulator with $3d^1$ configuration (i.e., one d electron per Ti site). In fact, a fairly stoichiometric compound of $LaTiO_3$ shows an insulating behavior accompanying the antiferrromagnetically spin-ordered phase below ca. 140 K.[4–6] Such an insulating and spin-ordered phase is unstable against the carrier doping (or change of the band filling), as reported previously[4–6] and also here in detail, which is analogous to the case of the doped cuprate compounds. Therefore, it is interesting to compare the electronic and magnetic phase diagrams as a function of the doping level for the titanate and cuprate systems. In addition to the nature of the charge gap (Mott vs CT type), there may be important differences in electronic structures and properties which originate from the dimension (D) of the systems (3D vs 2D).

In this paper, we report on the doping- and pressure-induced changes of electrical and magnetic properties in the $LaTiO_3$ system. The band filling or the concentration of the nominally doped "holes" can be finely varied by controlling slight nonstoichiometry or composition of Sr-doped $LaTiO_3$. We have clarified the electronic and magnetic diagram in the $LaTiO_3$ system as a function of the "hole" concentration. To see the dependence of the electronic properties on electron correlations, the effect of high pressure has been also investigated for the compounds near the Mott insulator-metal phase boundary. Application of high pressure tends to increase the one-electron bandwidth and hence decrease the electron correlation effect, while keeping the band filling. On the basis of these experimental data, we can argue the critical change of electronic and magnetic states in the Mott-insulating and barely metallic compounds as a function of both parameters, i.e., the correlation strength and band filling.

II. EXPERIMENTAL

All the samples investigated were prepared by the floating zone method. Starting materials were Ti, TiO_2, La_2O_3, and $SrTiO_3$. La_2O_3 and TiO_2 were well dried by firing at 1000°C in air before their use. As a dopant source, $SrTiO_3$ was synthesized by firing stoichiometric mixture of $SrCO_3$ and TiO_2 at 1150°C in air for 24 h. Ti, TiO_2, La_2O_3, and $SrTiO_3$ were weighed to a prescribed ratio of $LaTiO_{2.94}$ and $La_{0.95}Sr_{0.05}TiO_{2.94}$. Each mixture was pressed into two rods (5 mm in diameter and 20 mm and 100 mm in length). The bar-shaped in-

TABLE I. Characterization of each sample $La_{1-x}Sr_xTiO_{3+y}$

	Insulating		Metal-insulator		Metallic
	Sample A	Sample B			Sample C
x	0	0	0	0	0.05
y	0.00_7[a]	0.02_0[a]	0.02_3[a]	0.03	0.04
"hole" conc. δ	0.01	0.04	0.05	0.06	0.13
T_c (K)	138	118	114	93	
ρ (Ω cm) at 5 K	2×10^{3}	7×10^{-1}	3×10^{-2}	4×10^{-4}	6×10^{-3}
at 300 K	4×10^{-1}	2×10^{-2}	1×10^{-2}	2×10^{-3}	5×10^{-4}

[a] The errors are about ± 0.003.

gredients were melted (without further sintering) under Ar/H_2 atmosphere with use of a floating zone furnace equipped with two halogen incandescent lamps and double focusing mirrors. Nominally stoichiometric $LaTiO_3$ compounds (hereafter referred to as samples A and B) were synthesized in different reducing conditions: in gas flow of 30% H_2/Ar for sample A and of 18% H_2/Ar for sample B. On the other hand, the 5% Sr-doped sample $La_{0.95}Sr_{0.05}TiO_3$ (referred to as sample C) was synthesized in gas flow of 7% H_2/Ar. The feed rod and melt-grown part were rotated at 30 rpm and 20 rpm in opposite directions. The traveling speed of the melted zone was set rather high, at ca. 30 mm/h for samples A and B, and at ca. 60 mm/h for sample C to avoid a possible gradient of the composition due to the segregation effect.

All the samples show an orthorhombically distorted perovskite structure, or the so-called $GdFeO_3$-type structure.[7,8] Difference in lattice parameters of samples A and B (both nominal $LaTiO_3$) is hardly discernible within the resolution ($\sim$ 0.002 Å) of the present x-ray powder diffraction measurement. The stoichiometry of each sample was examined by thermogravimetric analysis (TGA). The results are shown in Table I together with electrical and magnetic properties (*vide infra*) for each sample. In the table, nonstoichiometry is assumed to be due to the oxygen nonstoichiometry in the formula of $La_{1-x}Sr_xTiO_{3+y}$. (The TGA measurements alone cannot determine whether the deviation of the Ti valence is due to oxygen nonstoichiometry or La deficiency.) Note that sample A ($x = 0$, $y = 0.007 \pm 0.003$; denoted hereafter $y = 0.00_7$) which was synthesized in a stronger reducing condition is better stoichiometric than sample B ($x = 0, y = 0.02$). The effective Ti valence (v) and the filling (n) of the $3d$ electron band can be given by the relations, $v = 3 + x + 2y$ and $n = 1 - x - 2y$, respectively. In other words, nonstoichiometry as well as Sr doping can nominally introduce "holes" with concentration δ ($= x + 2y$) in the Mott-Hubbard insulator $LaTiO_3$.

Resistivity measurements were carried out for each sample for the temperature range from 4.2 K to room temperature at various pressures up to 2.0 GPa. The pseudo-hydrostatic pressure was generated in a Teflon cell with a pressure transmitting fluid (Fluorinert No. FC70) using a WC piston-cylinder apparatus. The pressure was changed at room temperature, and held constant in the whole range of temperature with use of the constant load generating system. The pressure was determined by measuring the shift of the superconducting transition temperature of the lead manometer. The temperature was measured with a calibrated platinum-cobalt resistance thermometer attached adjacently to the sample cell. The temperature sweeps were set at a rate slower than 0.4 K/min to ensure thermal equilibration of the pressure apparatus.

Magnetic measurements were carried out with a superconducting quantum interference device (SQUID) magnetometer at ambient pressure. The magnetic susceptibility was measured in a field-cooled run with an applied field of 10^4 Oe down to 5 K. Then, the field was reduced to 100 Oe and the magnetization was measured in the heating run to determine the critical temperature for the weakly ferromagnetic phase transition.

III. DOPING-INDUCED CHANGES IN RESISTIVITY AND MAGNETIC SUSCEPTIBILITY

We show in Fig. 1 the temperature dependence of (a) resistivity and (b) magnetic susceptibility for $LaTiO_3$ (samples A and B) and partly Sr-substituted crystal $La_{0.95}Sr_{0.05}TiO_3$ (sample C).

The difference in the electronic and magnetic properties of these samples likely arises from a slight difference in the effective Ti valence or the band filling due to a change in stoichiometry, as indicated in Table I. (In the table, we include the parameters for the samples other than the A, B, and C samples.) Hereafter, we will refer to each sample also by its deviation (δ) of the Ti-valence ($3 + \delta$) or the concentration of nominally doped "holes" per Ti site. The band filling is given by the relation $n = 1 - \delta$. $LaTiO_3$ (A) with $\delta = 0.01$ shows a semiconducting behavior at all temperature below room temperature. On the other hand, sample B with $\delta = 0.04$ shows a metallic behavior, i.e., $d\rho/dT > 0$, above ca. 140 K, and then its resistivity shows an upturn below ca. 140 K. Such an apparent metal-semiconductor transition can be ascribed to the onset of the magnetically ordered phase, as will be shown later. Contrary to these cases, the 5% Sr-doped sample (C) with $\delta = 0.13$ shows a metallic behavior down to the lowest temperature. The temperature dependence of resistivity below ca. 170 K in sample C well obeys the T-squaric relation, $\rho = \rho_0 + AT^2$, where the coefficient A is ca. $2.3 \times 10^{-9}\,\Omega\,\mathrm{cm/K^2}$ (*vide infra*, see also Fig. 5). Such a T^2 dependence of resistivity at low temperature is observed in the whole metallic phase

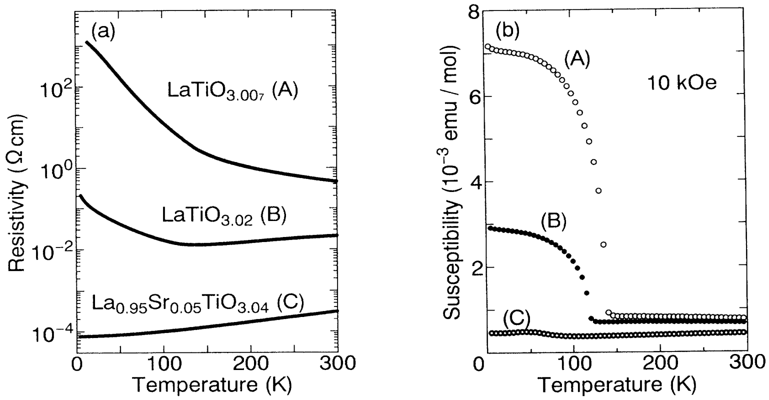

FIG. 1. Temperature dependence of (a) resistivity and (b) magnetic susceptibility in $LaTiO_{3+\delta/2}$ (samples A and B) and $La_{0.95}Sr_{0.05}TiO_{3.04}$ (sample C). The nominal hole concentration δ is 0.01 (A), 0.04 (B), and 0.13 (C).

of $La_{1-x}Sr_xTiO_3$ for $x \geq 0.05$.[5]

A drastic change in electronic states with the filling also manifests itself in the change in magnetic properties. The magnetic susceptibility for the respective samples A, B, and C [Fig. 1(b)] was measured for the same specimens that were investigated by transport measurements [Fig. 1(a)]. For the metallic sample C ($\delta = 0.13$), a nearly temperature-independent susceptibility was observed over the whole temperature region, being reminiscent of the Pauli paramagnetism. For samples A and B, a nearly temperature-independent susceptibility is also observed above ca. 150 K with an enhanced magnitude as compared with that of sample C. However, an abrupt increase in the susceptibility is observed with lowering temperature below ca. 138 K and ca. 118 K, respectively. This has been attributed to the phase onset of the weak ferromagnetism,[11] in which the spins on the Ti sites order antiferromagnetically with a small canting angle ($< 1°$). Judging from the *M-H* curve at low temperatures, the magnetization is nearly saturated at 1 T for samples A and B. Assuming that the canting angle is unchanged in samples A and B, a difference in saturated moments in the respective samples at the lowest temperature may be due to a doping-induced change in the magnitude of the effective moment in the antiferromagnetic phase.

We show in Fig. 2 and Fig. 3 observed correlations between the critical temperature (T_c) for the magnetic phase transition and the resistivity behavior for samples A and B, respectively. To determine T_c accurately, the magnetization (M) was measured with a weak field (100 Oe). The onsets of M are quite clear-cut for both cases, as shown in Figs. 2 and 3, which ensures that each compound is fairly homogeneous and nearly free from a phase mixture. The observed T_c's are 138 K and 118 K for samples A and B, respectively (see Table I). These values are consistent with those in the literature,[4,9–12] which are ranging from 120 K to 150 K perhaps depending on the δ value of the sample investigated. Concerning the stoichiometric homogeneity of the presently synthesized samples, it is worth mentioning the fact that the T_c values were well controllable and reproducible as far as the synthetic atmosphere, i.e., the $[H_2]/[Ar]$ ratio, was accurately controlled.

The magnetically ordered spins and the charge carriers arise from the identical Ti $3d$ electrons and hence the transport properties should be strongly correlated with the magnetic phase transition. In accord with this expectation, the inflection point of the ρ-T curve, e.g., a peak position of the $d^2\rho/dT^2$ curve, coincides quite well with T_c for *all* the samples with the spin-ordered phase listed in Table I. (The example is later shown in Fig. 3 for sample B.) For the insulating sample $LaTiO_{3.007}$ (sample A, $\delta = 0.01$), however, we would rather use here the quantity $d(\ln \sigma)/d(1/T)$ to show the correlation between σ and T_c, since the quantity can stand for the *apparent* activation energy of the electrical conduction in the form of $\sigma \sim \exp(\Delta/k_BT)$. The result is shown in Fig. 2 in comparison with the magnetization curve. The apparent activation energy for the electrical conduction above T_c is 450–480 K ($\sim$ 0.04 eV), but shows an abrupt change around T_c. Below T_c, the electrical conduction cannot be described by the activation-type formula, since the quantity, $d(\ln \rho)/d(1/T)$, remarkably decreases with lowering temperature. Reversibly, we can determine T_c by monitoring a jump of the apparent activation energy, as indicated by a vertical dotted line in Fig. 2.

For sample B ($\delta = 0.04$), which undergoes the metal-

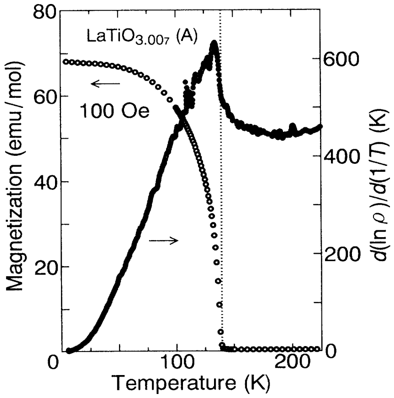

FIG. 2. Correlation between the resistivity change and magnetic phase transition in sample A ($\delta = 0.01$). The nominal activation energy Δ in units of K determined by $d(\ln \rho)/d(1/T)$ is plotted to be compared with the onset of the magnetization in the weak field (100 Oe) due to the spin-canted antiferromagnetic phase transition.

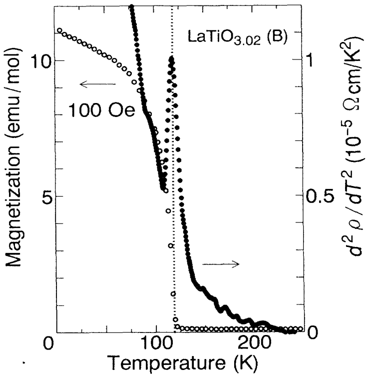

FIG. 3. Correlation between the resistivity change and magnetic phase transition in the sample B ($\delta = 0.04$). The second temperature derivative of resistivity is plotted to compare the onset of the magnetization in the weak field (100 Oe) due to the spin-canted antiferromagnetic phase transition.

nonmetal transition around 120 K, the second temperature derivative of resistivity $d^2\rho/dT^2$ is plotted in Fig. 3 to detect the anomaly upon the magnetic phase transition. A sharp peak of $d^2\rho/dT^2$ indicates a well-defined inflection point of the ρ-T curve, which precisely agrees with $T_c(=118$ K), as indicated by a vertical dotted line in Fig. 3. In previous papers,[12] it was argued that the resistivity upturn was nothing to do with the magnetic phase transition. The temperature at which the resistivity shows the minimum (i.e., $d\rho/dT = 0$) does not precisely coincide with $T_c(=118$ K), but the inflection temperature does. Thus, the transport properties in both the insulating and barely metallic LaTiO$_3$ compounds are strongly correlated with the spin states.

We have made similar measurements of transport and magnetic properties for the other LaTiO$_3$ samples with various δ values which were synthesized in different conditions, i.e., with varying [H$_2$]/[Ar] ratio. Part of these results are also included in Table I. On the basis of the experimental data,[6] we have drawn the electronic phase diagram in Fig. 4 as a function of δ (i.e., deviation of the band filling from $n = 1$). As seen in the figure, T_c decreases gradually with δ and then steeply at $\delta = 0.06 \sim 0.08$. We should note that the magnetically ordered phase below T_c changes its character critically with increase of δ. In particular, a remarkable reduction of the resistivity value in the magnetically ordered phase is observed with increase of δ as shown in Fig. 1 and Table I. For example, see the resistivity value at 5 K listed in Table I which changes from $\rho(5\text{ K}) = 4 \times 10^{-4}$ Ω cm for $\delta = 0.06$. This may indicate that the nature of the magnetism transits from localized to itinerant with increase of δ.

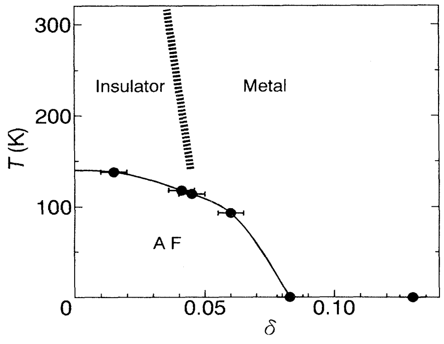

FIG. 4. Electronic and magnetic phase diagram in LaTiO$_{3+\delta/2}$ against change in the band filling (δ being the nominal hole concentration per Ti site). A.F. stands for the antiferromagnetically spin-ordered phase.

It is worth noting here that the observed phase diagram in carrier-doped titanates shows several common features to that for the cuprate superconductors, e.g., La$_{2-x}$Sr$_x$CuO$_4$ and Nd$_{2-x}$Ce$_x$CuO$_4$ systems.[13,14] They are, for example, presence of the antiferromagnetic spin (s=1/2) ordered phase at the end insulator, collapse of the magnetic phase and the insulator-metal transition with doping (change of the filling), etc. Apart from presence or absence of the superconducting phase, however, we should note an important difference between the doped titanates and cuprates: To be precise, δ in the case of the "doped" titanates cannot be interpreted as concentration of doped holes, since the Hall coefficient is always a negative characteristic of electron-type carriers and furthermore its magnitude is not so large as δ^{-1} in the whole metallic region even very close to the metal-nonmetal phase boundary.[6] This is in contrast with the fact that in the low-δ region(< 0.1) the layered cuprate compounds always show a positive (for the hole-doped case) or negative (for the electron-doped case) Hall coefficient of the order of δ^{-1}. Further detailed discussion of the barely metallic phase in comparison with the case of the cuprates will be published elsewhere, and in the following let us focus on the pressure effect on the electronic phase diagram shown in Fig. 4.

IV. VARIATION OF PRESSURE EFFECT WITH THE DOPING LEVEL

A. Pressure effect in the doping-induced metallic phase

First, let us discuss the effect of the hydrostatic pressure on the metallic sample C (La$_{0.95}$Sr$_{0.05}$TiO$_{3.04}$, δ = 0.13) to see what kind of electronic parameter is affected by the applied pressure. Temperature dependence of resistivity (ρ) is shown in Fig. 5(a) under various hydrostatic pressures, where ρ is plotted against the square of temperature (T^2). At least up to ca. 170 K ($T^2 \simeq 30\,000$ K^2), the resistivity can be well characterized by the relation, $\rho = \rho_0 + AT^2$, under high pressure as well, implying the strong electron-electron scattering process. However, the coefficient A decreases conspicuously with increasing pressure ($dA/dP = -2.8 \times 10^{-1}$ Ω cm/K^2 GPa), as shown in Fig. 5(b).

In previous studies,[5,15,16] we have observed the critical enhancement of the effective mass of carriers as the metallic La$_{1-x}$Sr$_x$TiO$_3$ approaches the end insula-

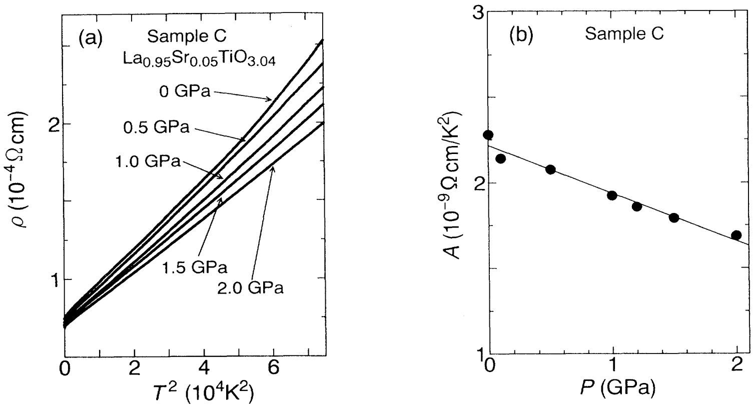

FIG. 5. (a) Temperature dependence of resistivity of sample C ($La_{0.95}Sr_{0.05}TiO_{3.04}$, $\delta = 0.13$) under pressures up to 2 GPa. (b) Pressure dependence of the T-squaric coefficient (A) of the metallic resistivity in sample C.

tor ($x \rightarrow 0$). In particular, the T-linear coefficient (γ) of the low-temperature specific heat becomes large in the metallic region vicinal to the end insulator. It has been found in a previous study[5] that the empirical relation, $A = b\gamma^2$, holds quite well in the metallic $La_{1-x}Sr_xTiO_3$ compounds ($0.7 \leq x \leq 0.95$), as in the other strongly correlated metals such as the heavy fermion systems.[17,18] The constant b is ca. $1.0 \times 10^{-5}\ \Omega\,\mathrm{cm}\,\mathrm{K}^2\,\mathrm{mol}^2\,\mathrm{J}^{-2}$ and coincides with the value reported for the heavy fermion systems. The results indicate that both the carrier mass and scattering rate are critically enhanced as δ decreases and the system approaches the end Mott-Hubbard insulator.

Assuming that the above empirical rule ($A = b\gamma^2$) holds good under pressures as well, we can estimate the pressure-induced change of γ or equivalently of the carrier effective mass (m^*):

$$\frac{1}{m^*}\frac{dm^*}{dP} = \frac{1}{\gamma}\frac{d\gamma}{dP} = \frac{1}{2A}\frac{dA}{dP} = -6.2 \times 10^{-11}\ \mathrm{Pa}^{-1}.$$

Namely, m^* decreases as much as 6.2% when the pressure of 1 GPa is applied. Such a pressure-induced decrease in m^* is attributable to the decrease in the effect of the electron correlation, which can be measured typically by the quantity U/W. (Here, U is the intra-atomic Coulombic repulsion and W the one-electron bandwidth.) The band filling $n(= 1 - \delta)$ is another important parameter which governs the effective strength of the electron correlation, yet δ is kept constant during the pressure measurement. Therefore, the most plausible effect of the applied pressure is to increase the one-electron bandwidth W and hence decrease the U/W value, since the pressure-induced change in lattice parameters is favorable for increasing the hopping interaction of the 3d electron.

B. Pressure effect on the magnetic phase transition

A similar increase in the one-electron bandwidth W is expected for sample A ($\delta = 0.01$) and sample B ($\delta = 0.04$) under pressure, since the lattice properties are expected to be nearly the same as sample C. The temperature dependence of the resistivity is plotted in Fig. 6(a) and Fig. 7(a) for samples A and B, respectively. For the insulating sample A, the resistivity is slightly decreased with pressure, yet remains still large under pressure. To see the change in more detail, we have plotted the quantity $d(\ln\rho)/d(1/T)$ as a function of T in Fig. 6(b) as was done in Fig. 2. A conspicuous shift of the λ-shaped feature is observed with pressure. As discussed in Fig. 2, the λ-shaped anomaly corresponds to the onset of the antiferromagnetic phase. Taking the positions of the anomalies shown in Fig. 6(a), we could accurately determine

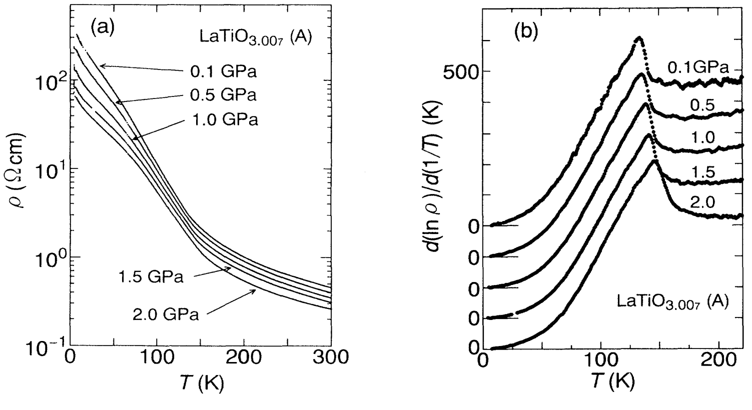

FIG. 6. Temperature dependence of (a) resistivity and (b) apparent activation energy $d(\ln\rho)/d(1/T)$ of sample A ($LaTiO_{3.007}$, $\delta = 0.01$) under pressures up to 2 GPa.

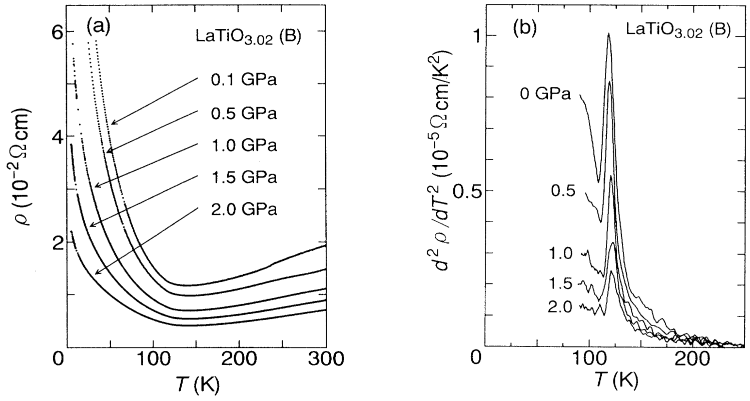

FIG. 7. Temperature dependence of (a) resistivity and (b) second temperature derivative of resistivity $d^2\rho/dT^2$ of sample B ($LaTiO_{3.02}$, $\delta = 0.04$) under pressures up to 2 GPa.

T_c of sample A under pressure. The result for sample A is shown in Fig. 8 by filled circles, which shows a fairly large increase in T_c at a rate of 6.8 K/GPa.

On the other hand, a more remarkable pressure effect was observed in the low-temperature resistivity of sample B ($\delta = 0.04$) [Fig. 7(a)] which undergoes the metal-nonmetal transition relating with the magnetic transition. The resistivity at 5 K is reduced by one order of magnitude with application of pressure of 2 GPa and the whole ρ-T curve appears to approach the metallic one with pressure. However, the metal-nonmetal transition temperature is rather insensitive to pressure. (Incidentally, a small anomaly around 240 K which shifts to higher temperature with pressure is due to effect of solidification of the pressure-transmitting fluid medium.)

In Fig. 7(b), the second temperature derivative of resistivity (see also Fig. 3) is shown for sample B. The temperature corresponding to a peak anomaly due to the onset of the antiferromagnetic phase is rather insensitive to pressure, but its magnitude is conspiciously reduced with pressure. The spin moment coupled with the conduction electron is perhaps reduced as the antiferromagetic phase below T_c changes its character from localized to itinerant with an increase of δ. In Fig. 8 we show the pressure dependence of T_c for sample B by assigning the peak position to T_c. The least-squares fit assuming the linear change of T_c indicates that $dT_c/dP = 2.3$ K/GPa. It is to be noted in Fig. 8 that there is a conspicuous difference in pressure coefficients of T_c in both $LaTiO_3$ compounds, sample A ($\delta = 0.01$) and sample B ($\delta = 0.04$): The coefficient for sample A is about three times larger than that for sample B, which is obviously originating from a difference in the filling parameter or δ value.

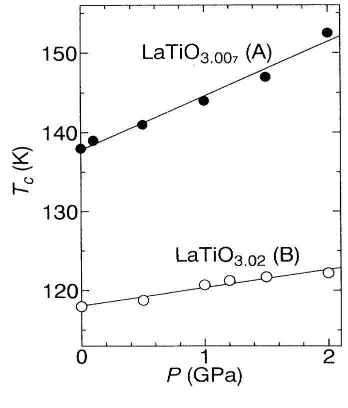

FIG. 8. Pressure dependence of the magnetic transition temperatures for $LaTiO_{3+\delta/2}$, sample A ($\delta = 0.01$), and sample B ($\delta = 0.04$).

As argued in the previous section, applied pressure likely tends to increase the one-electron bandwidth (W). Therefore, we should first consider the dependence of T_c on the effective strength of the electron correlation as measured by U/W. The prediction by the Heisenberg model and the random phase approximation (RPA) for the half-filled band should be valid in the very strong ($U/W \gg 1$) and very weak ($U/W \ll 1$) correlation regions, respectively.[19,20] In the case of the Heisenberg spin regime, the exchange interaction and hence T_c is expected to increase with the one-electron bandwidth as $\propto W^2/U$. By contrast, T_c would steeply decrease with W as $\propto W \exp[-1/D(E_F)U]$ in the case of the spin-density-wave phase where the RPA model holds good [$D(E_F)$ stands for the density of states at the Fermi level(E_F)]. Therefore, with increasing value of W/T_c from zero T_c should first increase as predicted by the Heisenberg model, then tend to saturate, and reach the maximum. In the region of the itinerant magnetism with further increase of W/U, T_c will rather decrease in accord with the RPA prediction.[19,20] In such a case, a pressure coefficient of T_c will be monotonously decreasing as a function of W/U from the positive to negative value, as far as we can consider that the primary effect of the applied pressure is to increase the W/U.

A positive pressure shift of T_c as observed in $LaTiO_{3+\delta}$ is in accord, at least qualitatively, with the behavior expected for the localized spin system. However, a remarkable reduction of the pressure coefficient of T_c with a slight increase of δ (e.g., by 0.04) may indicate a variation in the nature of the spin-orderd phase. In light of the above argument, the observed result can be interpreted as a symptomatic change in the magnetic nature from localized to itinerant (or less localized). Such a change is, of course, caused by a change of δ and not by that of W/U in the present system, though intuitively both cases are expected to be analogous to each other. For a more detailed analysis of the present result, we would need a theoretical model which can quantitatively describe the change of T_c in the parameter space of both W/U and δ.

V. CONCLUSION

We have investigated the doping- and pressure-induced change of electronic and magnetic properties in the Mott-Hubbard system $LaTiO_3$. Defining δ as the nominal hole concentration [or $n(=1-\delta)$ as the band filling], we have clarified the electronic and magnetic phase diagram as a function of δ in the $LaTiO_3$ system. Carrier doping (δ) or variation of the band filling (n) was done by controlling the slight nonstoichiometry or Sr doping. The Mott-insulating state is converted to the barely metallic state at high temperature (>150 K) for the doping level above $\delta = 0.02$, yet the magnetically ordered low-temperature phase persists up to $\delta = 0.08$ (see Fig. 4). However, the spin-ordered phase itself appears to gradually acquire the itinerant character with increase of δ, as revealed by the measurements of resistivity as well as of the pressure coefficient of the transition temperature. The situation is analogous to the doped cuprate compounds, in particular the electron-doped compounds $Nd_{2-x}Ce_xCuO_4$,[13,14] in which a similar crossover behavior of the magnetic properties has been observed with increasing doping level x.

ACKNOWLEDGMENTS

We are grateful to M. Imada and H. Fukuyama for enlightening discussion and to Y. Taguchi for his collaboration in high-pressure measurements. The work was supported by a Grant-In-Aid for Scientific Research from the Ministry of Education, Science and Culture, Japan.

---

[*] Author to whom correspondence should be addressed.

[1] J. B. Torrance, Y. Tokura, A. I. Nazzal, A. Bezinge, T. C. Huang, and S. S. Parkin, Phys. Rev. Lett. **61**, 1127 (1988).

[2] H. Takagi, S. Uchida, and Y. Tokura, Phys. Rev. Lett. **62**, 1197 (1989).

[3] J. Zaanen, G. A. Sawatzky, and J. W. Allen, Phys. Rev. Lett. **55**, 418 (1985); J. Solid State Chem. **88**, 8 (1990).

[4] F. Lichtenberg, D. Widmer, J. G. Bednorz, T. Williams, and A. Reller, Z. Phys. B **82**, 211 (1991).

[5] Y. Tokura, T. Taguchi, Y. Okada, Y. Fujishima, T. Arima, K. Kumagai, and Y. Iye, Phys. Rev. Lett. **70**, 2126 (1993).

[6] Y. Okada, Y. Tokura, and Y. Iye (unpublished).

[7] D. A. Maclean, Hok-Nam Ng, and J. E. Greedan, J. Solid State Chem. **30**, 35 (1979).

[8] J. E. Sunstrom IV, S. M. Kauzlarich, and P. Klavins, Chem. Mater. **4**, 346 (1992).

[9] D. A. MacLean and J. E. Greedan, Inorg. Chem. **20**, 1025 (1981).

[10] J. E. Greedan, J. Less-Common Met. **111**, 335 (1985).

[11] M. Eitel and J. E. Greedan, J. Less-Common Met. **116**, 95 (1986).

[12] D. A. Crandles, T. Timusk, and J. E. Greedan, Phys. Rev. B **44**, 13 250 (1991).

[13] S. Kambe, H. Yasuoka, H. Takagi, S. Uchida, and Y. Tokura, J. Phys. Soc. Jpn. **60**, 400 (1991).

[14] Y. J. Uemura *et al.*, Phys. Rev. Lett. **62**, 2317 (1989).

[15] Y. Fujishima, Y. Tokura, T. Arima, and S. Uchida, Phys. Rev. B **46**, 11 167 (1992).

[16] K. Kumagai, T. Suzuki, Y. Taguchi, Y. Okada, Y. Fujishima, and Y. Tokura, Phys. Rev. B **48**, 7636 (1993).

[17] K. Kadowaki and S. B. Woods, Solid State Commun. **55**, 507 (1986).

[18] K. Miyake, T. Matuura, and C. M. Varma, Solid State Commun. **71**, 1149 (1989).

[19] J. E. Hirsch, Phys. Rev. B **35**, 1851 (1987).

[20] T. Moriya and H. Hasegawa, J. Phys. Soc. Jpn. **48**, 1490 (1980); in *Electron Correlation and Magnetism in Narrow-Band Systems*, edited by T. Moriya (Springer, New York, 1981).